Surface-enhanced Raman scattering from rhodamine 6G on gold-coated self-organized silicon nanopyramidal array

Rui Li, Hong Li, Shi Pan,[a] Kun Liu, Shanshan Hu, Lujun Pan, Yingnan Guo, and Shifa Wu
Institute of Near-Field Optics & Nano Technology, School of Physics and Optoelectronic Technology, Dalian University of Technology, Dalian 116024, People's Republic of China

Xufeng Li
School of Applied Science, Taiyuan University of Science and Technology, Shanxi 030024, China

Jun Liu
Microelectronics and Solid State Electronics, School of Physics and Optoelectronic Technology, Dalian University of Technology, Dalian 116024, People's Republic of China

(Received 17 July 2013; accepted 12 November 2013)

This work reports the gold-coated self-organized silicon nanopyramidal array prepared by a wet etching and magnetron sputtering process at room temperature. Scanning electron microscopy was used to detect the morphology of gold films. The surface-enhanced Raman scattering (SERS) spectra of the rhodamine 6G (R6G) molecules adsorbed on a nanoscale gold film were recorded. Experimental results show the relationships between gold film thickness and SERS intensity. A full three-dimensional finite difference time domain calculations were carried out, which compare the experimental results and show agreement with ratios of the SERS enhancement for the different thicknesses of gold films. Furthermore, numerical simulations of the array were conducted for both a real gold metal coating and a perfect electrical conductor to determine whether the SERS enhancement was due to diffraction or plasmonic effects. The sample with the fast fabrication process used in this work could provide a new way to obtain a uniform enhancement and low cost SERS substrate.

I. INTRODUCTION

In the past decade, surface-enhanced Raman scattering (SERS), which was first observed by Fleischmann et al.,[1] for molecules adsorbed on the metal surface, has been widely applied in single molecule detection,[2] surface chemistry,[3] cancer detection,[4] material analysis,[5] etc. In SERS, electromagnetic enhancement (EME) and chemical enhancement (CE) are two primary mechanisms. The EME is based on the resonant excitation of localized surface plasmons and is correlated with the physical characteristics of the metal nanostructures, whereas the CE involves charge transfer due to the chemisorption of the analyte. It is notable that the SERS enhancement factor (EF) combining EME with CE can reach the 10^{10}–10^{11} range.[6]

The basic principle in manufacturing SERS-active substrates lies on the spatially localized regions of strongly enhanced local electromagnetic fields (named "hot spot") of a nanostructured surface or nanoparticle.[7] A number of promising nanostructures have been developed for creating hot spots, such as nanoparticles,[2,8] nanorods,[9] nanocrystal,[10,11] and other special nanostructures (nanorice, nanocrescent, nanobowl, single nanowire, tip enhancement, etc).[12–16] In addition to these structures, a series of metals have been used to obtain surface enhancement, where gold, silver, and copper were commonly used in surface enhancement. However, due to the reasonable chemical stability, gold was widely used.

Along with the development of nanofabrication, nanoscaled periodic SERS substrates have been made with anisotropic wet etching,[17] photolithography, e-beam lithography,[18] self-assembly,[19] deep reactive ion etching,[20] nanoimprint,[21,22] vapor deposition, etc. It was reported that silver films over a periodic nanosphere substrate show the best average EF of about 4.3×10^6 (Ref. 23); gold-coated periodic pyramidal substrates prepared by a nanoimprint process show the average EF of 7.2×10^4 for pyramidal tip substrates and 1.6×10^6 for pyramidal pit substrates.[24] There are also some other reports on gold-coated periodic pyramidal substrates.[25–27] Compared with the periodic pyramidal structures, self-organized structures are more realistic, effective, cost-effective, and time-saving, but the controllability is much lower.

We have developed a very simple process to prepare self-organized gold-coated silicon nanopyramidal arrays for sensitive detection of Raman signal uniformly, which have potential usage for large scale and low cost fabrication of SERS substrates. To accurately model both the

[a]Address all correspondence to this author.
e-mail: span@dlut.edu.cn
DOI: 10.1557/jmr.2013.352

 © Materials Research Society 2013

https://doi.org/10.1557/jmr.2013.352 Published online by Cambridge University Press

density and distribution of electric field on the nanopyramidal array, a 3D model for the positive square-based nanopyramid pattern was explored by using 3D-finite difference time-domain (3D-FDTD) simulation. To investigate the physical mechanism for the SERS signal enhancement, the nanopyramids coated with a gold film and a PEC film were used in our simulation. It was concluded that the gold film thickness played a major role in the SERS enhancement.

II. EXPERIMENTAL

A. Instrumentation

Scanning electron microscope (SEM) images were taken by the FEI Nova NanoSEM 450 SEM system (Hillsboro, OR). Raman spectrum was recorded at room temperature by a Renishaw inVia Raman microscope spectrometer (Gloucestershire, UK). Spectra were collected over the range of 500–1800 cm^{-1}. A He–Ne visible laser with a wave length of 632.8 nm and a power of 2.2 mW was used as the excitation source. The excitation light is delivered and the backscattered light was collected by a 50 × 0.55 NA objective lens (Nikon Inc., Tokyo, Japan). A miniature ion-sputtering instrument SBC-12 (KYKY Technology Co., Beijing, China) was used for metal evaporation.

B. Sample preparation

A 3D sketch for the fabrication of gold-coated silicon pyramidal substrates is shown in Fig. 1. Native oxide on the Si wafer surface was removed by diluted hydrogen fluoride (HF) (49%) solution ($HF:H_2O$ = 1:10) at first. Positive Si pyramidal substrates were prepared by anisotropic wet etching of (111) crystalline planes of the (100) Si wafer at 70 °C for 30 min in a fresh solution containing [KOH (g):IPA (mL):DI water (mL) = 0.5:0.65:37.5]. Then, the substrates were rinsed with DI water for 10 min and dried in air for 20 min followed by the deposition of gold films on the prepared silicon nanopyramids with thicknesses of 25–150 nm.

One important application of SERS substrate was detecting low concentration molecules and biomolecules with ultrahigh sensitivity. For a better understanding of the effects of gold film thickness on EME, R6G molecules (Sigma Aldrich, St. Louis, MO) were used as the analyte for testing its detection sensitivity. R6G molecules were adsorbed on the gold film by horizontally immersing the substrates in R6G (10^{-7} M) solution at room temperature for 12 h and then drying in the air. To ensure the repeatability and reliability of the measured results, we took multiple measurements at the same location and averaged the spectra on each sample.

III. RESULTS AND DISCUSSION

A SEM image of the silicon pyramidal substrate with the pyramidal faces at an angle of 35.3° from the surface normal was shown in Fig. 2(a). To avoid oxidization of the metal, a thin gold film was deposited on the substrates by magnetron sputtering. The inseted image in Fig. 2(a) shows a high-resolution SEM image of the self-organized silicon nanopyramidal array coated with a gold film. Numerous gold intersecting lines can be observed among the nanopyramids. It was also found from the inseted image that there were a large amount of cracks in the gold film covered on the surface of the silicon pyramidal substrate. These cracks, having widths of the nanometer scale, were self-organized during the deposition process because of oblique angle deposition,[28] which was not found in the smooth surface of a normal silicon substrate. These sharp nanocracks in the gold film are regarded as the "hot-spots" of SERS.[29] As shown in Fig. 2(b), the bar chart depicts the distribution character of pyramidal nanostructures with various base lengths. Left (black) bars indicate the distribution by quantity, and right (green) bars indicate the projected area distribution.

Figure 3 shows a series of SERS spectra for R6G (10^{-7} M) adsorbed on gold-coated substrates with different gold thicknesses ranging from 25 to 125 nm gold-coated polished silicon substrates. The positions and relative amplitude of these spectra agree well with the previous results.[30] The band at approximately 613 cm^{-1} is assigned to the C–C–C ring in-plane vibration mode. The band at approximately 772 cm^{-1} is assigned to the C–H out-of-plane bend mode. The bands at approximately 1126 and 1185 cm^{-1} are assigned to the C–H in-plane bend modes. The bands at approximately 1312 and 1575 cm^{-1} are assigned to the N–H in-plane bend modes. The bands at approximately 1362, 1510, and 1648 cm^{-1} are assigned to the C–C stretching modes.[30] It is noted that there is no R6G signal from the gold-coated flat silicon substrate due to insufficient coupling between the incident field and the gold surface, whereas R6G SERS signal can be observed

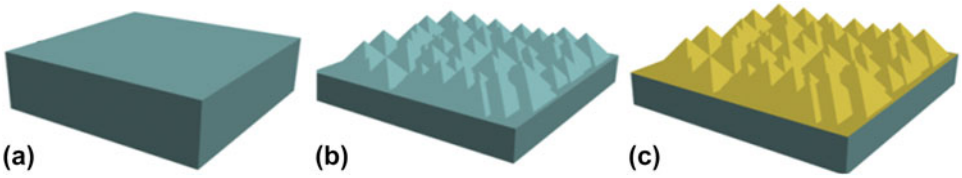


FIG. 1. Fabricate sketch of gold-coated silicon pyramidal substrates. (a) Crystalline silicon was cleaned with piranha and dilution HF; (b) Si pyramids were formatted by anisotropic wet etching in the KOH/IPA solution; (c) gold film was deposited on silicon pyramidal substrates.

https://doi.org/10.1557/jmr.2013.352 Published online by Cambridge University Press

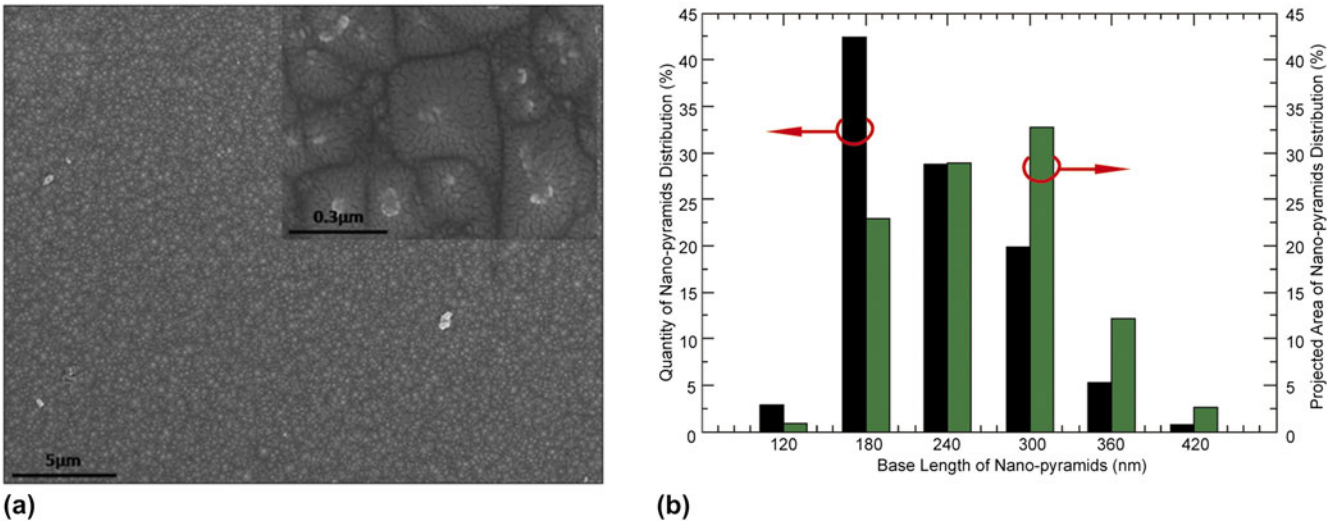


FIG. 2. (a) SEM image of the silicon pyramidal nanostructure coated with a 75-nm gold film on the surface. The inset is an enlarged SEM image. (b) Bar chart showing the distribution character of pyramidal nanostructures with various base lengths. Left (black) bars indicate the distribution by quantity; right (green) bars projected area distribution.

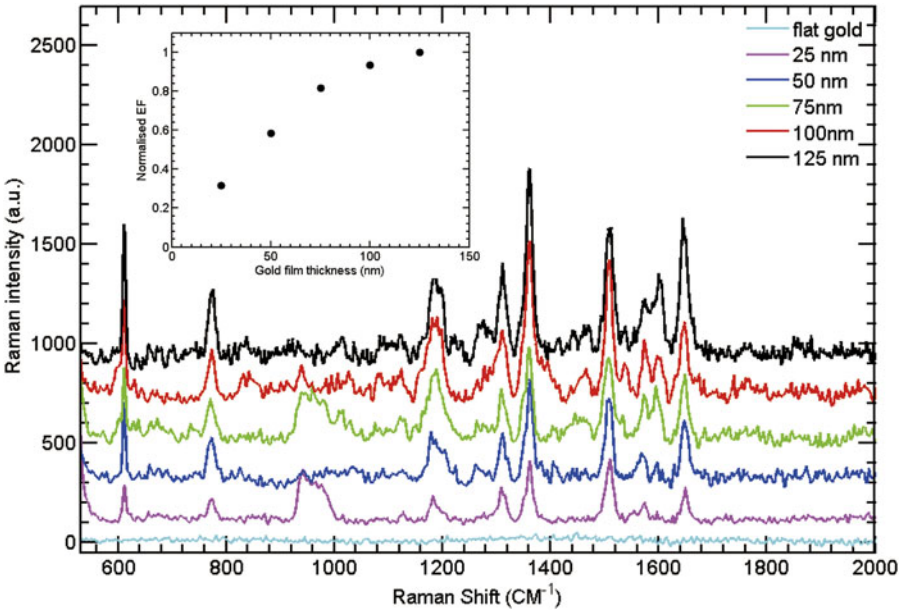


FIG. 3. SERS spectra of R6G (10^{-7} M) obtained on the silicon pyramidal substrate coated with different thicknesses of gold film and the gold-coated polished silicon substrate, respectively. The spectra were taken under 632.8-nm He–Ne laser at 2.2 mW with an integration time of 10 s. Thicknesses of gold films are from 25 to 125 nm, increased by a step of 25 nm on silicon pyramidal substrates and 125 nm on gold coated polished silicon substrates. The inset chart is the normalized EF of the nanopyramid substrate with different gold film thicknesses of 25, 50, 75, 100, and 125 nm.

obviously from the sample of gold-coated silicon pyramidal substrates.

Following the deposition of various thicknesses of gold films on the silicon pyramidal substrates, a significant enhancement in the SERS signal is observed (Fig. 3). It is found that the SERS signal increases with increasing the thickness of the gold film. However, the SERS signal tends to be saturated after the thickness of the gold film reaches 100 nm.

The EF for the gold-coated pyramidal array is calculated by comparing the intensity of the R6G major characteristic Raman peak at approximately 1362 cm^{-1}. The Raman signal from R6G molecules adsorbed on a polished silicon wafer by immersing the substrates in R6G (10^{-2} M) solution at room temperature for 12 h and then drying in the air was used as the reference. To obtain the precise intensity of the Raman peak, the cubic spline interpolation fitting was used to remove the fluorescence baseline. We attempted to estimate the SERS EF using the following equation[31]:

https://doi.org/10.1557/jmr.2013.352 Published online by Cambridge University Press

$$\mathrm{EF} = (I_{\mathrm{SERS}}/N_{\mathrm{SERS}})/(I_{\mathrm{NR}}/N_{\mathrm{NR}}) \quad , \qquad (1)$$

where I_{SERS} denotes the SERS intensity of R6G characteristic peak, I_{NR} denotes the normal Raman scattering intensity of the same peak. N_{SERS} and N_{NR} are the numbers of R6G molecules effectively excited by the laser beam to obtain the corresponding SERS and normal Raman spectra, respectively. The EF of the 125-nm gold-coated pyramidal substrate was estimated to be 3.8×10^5.

Numerical simulations were used to investigate the electric field enhancement of the gold-coated silicon pyramidal substrate using a 3D-FDTD method. The basic principle is that the structure is discrete into a number of cube cells, which are the so-called Yee cells. The FDTD method aims at solving Maxwell's equations from cell to cell in time domain.[32] The frequency dispersions of Si and gold permittivities in all simulations have been taken from Palik.[33] Positive silicon pyramidal arrays coated with gold films were modeled as a SERS substrate, with the film thickness adjusted. A transverse electric (TE)-polarized plane wave with a wave length of 632.8 nm is normally incident onto the top of the sample ($|E_0| = 1$). For the shape domains, the mesh size of the intersecting line between two pyramidal areas was $1 \times 1 \times 1$ nm^3 in the x–y–z space for better accuracy. Perfectly matched layers were adopted both up and down to avoid artificial reflections while periodic boundary conditions (PBCs) have been applied; introduction of these boundary conditions is equivalent to considering an infinite nanopyramid.

Figure 4 shows the calculated results of electric field distribution around the periodic adjacent nanopyramids with a base length of $D = 300$ nm. During the simulation, two plane monitors are set at $x = 0$ nm crossing the array of the nanopyramids and another at $y = 0$ nm crossing the intersection of two nanopyramids to detect the electric field intensity distribution, respectively. The total electric field intensity is defined as $|E_{\mathrm{tot}}|^2 = |E_x|^2 + |E_y|^2 + |E_z|^2$.

The z-plane and x-plane cross-sectional views of electric field intensity profiles for a gold-coated silicon pyramidal substrate were shown in Figs. 4 (c) and 4(d), respectively. The surface charges on the walls of the nanopyramids relate to the polarization of the incident electric field. These places would have two kinds of opposite charges on two adjacent walls. Due to the opposite charges getting close to each other while approaching the line of intersection, strong localized plasmons are formed.[34] A strong electric field profile with the maximum above the intersecting line of two nanopyramids is shown in Fig. 4(c). The intersecting line between the two nanopyramids was named "hot line," which plays the same role as hot spots [Fig. 4(d)].[29] A hot line can be assumed to be composed of an infinite number of hot spots (Fig. S1). Compared with the randomly dispersed hot spots, the stability and uniformity of the SERS signal from the molecules adsorbed on the numerous hot lines formed among the nanopyramids would be largely improved, which agrees well with our Raman mapping results in Fig. 6 in the following research.

The influence of gold thickness on the electric field intensity on the surface of the gold-coated silicon substrate has also been investigated. Hot lines on the gold-coated silicon pyramidal substrate exhibit a strong contribution to the SERS signal arising from the strong localized plasmons because that the gold film can couple the plasmons to hot line [Figs. 4(c) and 5]. The thickness of the gold film influences the penetration depth of surface plasmons in the gold film. As shown in Fig. 5, the electric field intensity along a hot line is investigated for

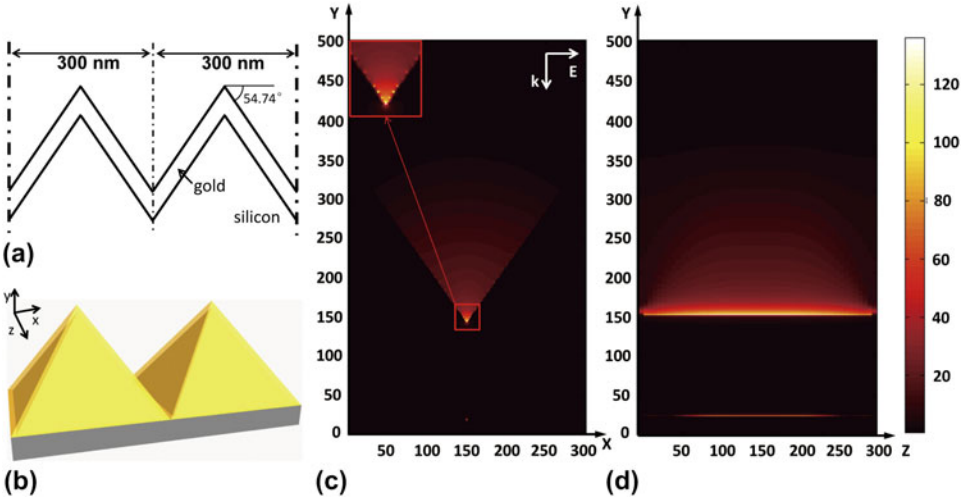


FIG. 4. (a) 2D cross section through the nanopyramid, the base length is 300 nm; (b) 3D schematic view of electric field distribution of SERS-active substrate, which has the same base length of 300 nm, coated with 125-nm gold film. The electric field distribution is simulated by 3D-FDTD under 632.8-nm excitation, the arrow indicates the polarization of the incident light [(c) is plane $z = 150$ nm and (d) is plane $x = 0$ nm].

https://doi.org/10.1557/jmr.2013.352 Published online by Cambridge University Press

the thickness ranging from 20 to 200 nm. The electric field intensity changes smoothly as the gold film thickness increases, and the intensities have the same tendency as the thickness varied [show in Fig. 5(b)]. While, for the film thicknesses greater than 100 nm, the hot spot signals obtained from three nanopyramids with different base lengths are approximately constant. The simulated result is consistent with our Raman experimental results in Fig. 5(a) (dots).

For a better understanding of the overall physical mechanism, we used a perfect electric conductor (PEC) film in place of the gold layer.[34] The electric field intensity for the PEC appears constant as the film thickness is increased [Fig. 5(a)]. The result for the gold layer differs significantly from the PEC layer, which is considered to be the plasmonic coupling effects that became dominant for thicker film and causes the EF of the SERS signal[34] (Fig. S2). According to the experimental and calculated results, the SERS observed from the gold-coated silicon pyramidal substrates should be a combined effect of the hot spots that arise from the nanocracks of the gold film and the hot lines that arise from the intersection among the adjacent gold-coated silicon nanopyramids.

As shown in Fig. 6, the Raman mapping[35] (1-μm step size, $11 \times 13 = 143$ spectral lines in all) was measured to test the uniformity and reproducibility of the 125-nm gold-coated silicon pyramidal substrate with R6G (10^{-7} M) as the target analyte. Figure 4 displays the top view of the Raman mapping spectra, from which we can see that all 143 spectral lines reveal stable R6G characteristic peaks. The standard deviation of the spectral intensity at 613 cm^{-1} for all the recorded spectral lines ($n = 143$) is 24.3%, demonstrating an outstanding uniformity and reproducibility of the SERS substrate.

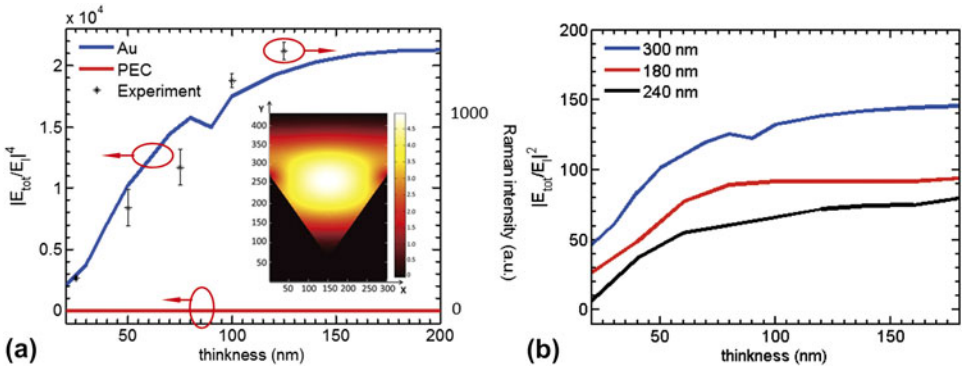


FIG. 5. (a) Simulated results show electric field intensity $|E|4$ versus the thickness of gold film for the same nanostructure, and the dependence of SERS intensity at 1362 cm^{-1} on the gold-coated silicon pyramidal substrate (dot). The inset is a cross-sectional view of the electric field distribution for the SERS-active substrate coated with the PEC film. (b) Raman intensities versus gold film thicknesses. The base length is illustrated by different colors from 180 to 300 nm.

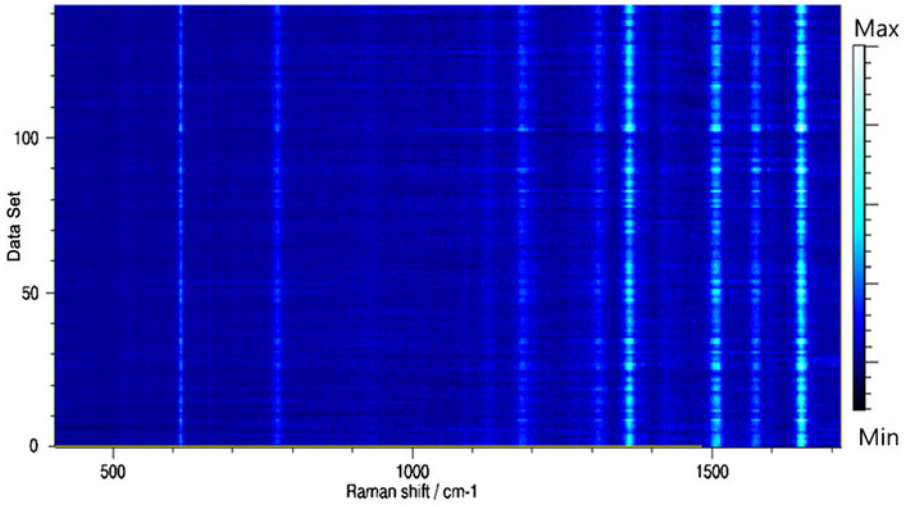


FIG. 6. Top view of SERS spectra measured from a probed volume that contains R6G molecules attached to a gold film on the silicon pyramidal substrate.

https://doi.org/10.1557/jmr.2013.352 Published online by Cambridge University Press

IV. CONCLUSIONS

The gold-coated self-organized nanopyramdial array has been fabricated for the first time by a simple wet etching and magnetron sputtering method and exhibited a high SERS signal enhancement. The EF of this structure is obtained to be 3.8×10^5 when the gold film thickness was 125 nm with 632.8-nm excitation. The 3D-FDTD calculations for the different configurations give values in reasonable agreement with experimental results. The uniform SERS EF attributed to the plasmonic coupling effect is confirmed by calculation via comparing gold and PEC films with the same thickness coated on the identical nanopyramids. The simulation result also reveals that, for this gold film-decorated pyramidal array, the largest electric field is mainly produced along the line of intersection, forming continuous and abundant hot spots for SERS enhancement. With this maskless process, the SERS substrate can be produced with excellent properties of easy fabrication, low cost, and uniformity.

ACKNOWLEDGMENTS

Project supported by the National Natural Science Foundation of China (Grant Nos. 10974025, 11074029, and 61137005) and the Fundamental Research Funds for the Central Universities of China DUT13ZD107 and DUT13LK21. RL acknowledges CSC scholarship funding for financial support. The authors also acknowledge help and support from P.F. Ji, Y. Wan, Matt, and Emily on this project.

REFERENCES

1. M. Fleischm, P.J. Hendra, and A.J. McQuilla: Raman spectra of pyridine adsorbed at a silver electrode. *Chem. Phys. Lett.* **26**(2), 163 (1974).
2. S.M. Nie and S.R. Emery: Probing single molecules and single nanoparticles by surface-enhanced Raman scattering. *Science* **275**(5303), 1102 (1997).
3. F. Eftekhari, A. Lee, E. Kumacheva, and A.S. Helmy: Examining metal nanoparticle surface chemistry using hollow-core, photonic-crystal, fiber-assisted SERS. *Opt. Lett.* **37**(4), 680 (2012).
4. K.K. Maiti, U.S. Dinish, C.Y. Fu, J-J. Lee, K-S. Soh, S-W. Yun, R. Bhuvaneswari, M. Olivo, and Y-T. Chang: Development of biocompatible SERS nanotag with increased stability by chemisorption of reporter molecule for in vivo cancer detection. *Biosens. Bioelectron.* **26**(2), 398 (2010).
5. L.H. Oakley, S.A. Dinehart, S.A. Svoboda, and K.L. Wustholz: Identification of organic materials in historic oil paintings using correlated extractionless surface-enhanced Raman scattering and fluorescence microscopy. *Anal. Chem.* **83**(11), 3986 (2011).
6. H.X. Xu, J. Aizpurua, M. Kall, and P. Apell: Electromagnetic contributions to single-molecule sensitivity in surface-enhanced Raman scattering. *Phys. Rev. E* **62**(3), 4318 (2000).
7. J.P. Camden, J.A. Dieringer, Y. Wang, D.J. Masiello, L.D. Marks, G.C. Schatz, and R.P. Van Duyne: Probing the structure of single-molecule surface-enhanced Raman scattering hot spots. *J. Am. Chem. Soc.* **130**(38), 12616 (2008).
8. W.E. Doering and S.M. Nie: Single-molecule and single-nanoparticle SERS: Examining the roles of surface active sites and chemical enhancement. *J. Phys. Chem. B* **106**(2), 311 (2002).
9. S. Shanmukh, L. Jones, J. Driskell, Y. Zhao, R. Dluhy, and R.A. Tripp: Rapid and sensitive detection of respiratory virus molecular signatures using a silver nanorod array SERS substrate. *Nano Lett.* **6**(11), 2630 (2006).
10. J.T. Krug, G.D. Wang, S.R. Emory, and S.M. Nie: Efficient Raman enhancement and intermittent light emission observed in single gold nanocrystals. *J. Am. Chem. Soc.* **121**(39), 9208 (1999).
11. J. Zhou, J. An, B. Tang, S. Xu, Y. Cao, B. Zhao, W. Xu, J. Chang, and J.R. Lombardi: Growth of tetrahedral silver nanocrystals in aqueous solution and their SERS enhancement. *Langmuir* **24**(18), 10407 (2008).
12. K. Li, L. Clime, B. Cui, and T. Veres: Surface enhanced Raman scattering on long-range ordered noble-metal nanocrescent arrays. *Nanotechnology* **19**(14), 145305 (2008).
13. J. Ye, L. Lagae, G. Maes, G. Borghs, and P. Van Dorpe: Symmetry breaking induced optical properties of gold open shell nanostructures. *Opt. Express* **17**(26), 23765 (2009).
14. Y. Huang, Y. Fang, and M. Sun: Remote excitation of surface-enhanced Raman scattering on single Au nanowire with quasi-spherical termini. *J. Phys. Chem. C* **115**(9), 3558 (2011).
15. Y. Wu, K. Liu, X. Li, and S. Pan: Integrate silver colloids with silicon nanowire arrays for surface-enhanced Raman scattering. *Nanotechnology* **22**(21), 215701 (2011).
16. M. Sun, Z. Zhang, H. Zheng, and H. Xu: In-situ plasmon-driven chemical reactions revealed by high vacuum tip-enhanced Raman spectroscopy. *Sci. Rep.* **2**, 647 (2012).
17. K.E. Bean: Anisotropic etching of silicon. *IEEE Trans. Electron Devices* **25**(10), 1185 (1978).
18. D. Bhandari, S.M. Wells, A. Polemi, I.I. Kravchenko, K.L. Shuford, and M.J. Sepaniak: Stamping plasmonic nanoarrays on SERS-supporting platforms. *J. Raman Spectrosc.* **42**(11), 1916 (2011).
19. Y.J. Liu, Z.Y. Zhang, R.A. Dluhy, and Y.P. Zhao: The SERS response of semiordered Ag nanorod arrays fabricated by template oblique angle deposition. *J. Raman Spectrosc.* **41**(10), 1112 (2010).
20. G. Das, F. Mecarini, F. Gentile, F. De Angelis, H.G. Mohan Kumar, P. Candeloro, C. Liberale, G. Cuda, and E. Di Fabrizio: Nano-patterned SERS substrate: Application for protein analysis vs. temperature. *Biosens. Bioelectron.* **24**(6), 1693 (2009).
21. R. Alvarez-Puebla, B. Cui, J-P. Bravo-Vasquez, T. Veres, and H. Fenniri: Nanoimprinted SERS-active substrates with tunable surface plasmon resonances. *J. Phys. Chem. C* **111**(18), 6720 (2007).
22. M.A. Vincenti, M. Grande, G.V. Bianco, D. de Ceglia, T. Stomeo, M. De Vittorio, V. Petruzzelli, G. Bruno, A. D'Orazio, and M. Scalora: Surface-enhanced Raman scattering from finite arrays of gold nano-patches. *J. Appl. Phys.* **113**(1), 013103-1-013103-5 (2013).
23. L. Wen-Chi, L. Lu-Shing, C. Yi-Hui, C. Hung-Chun, T. Din, and C. Hai-Pang: Size dependence of nanoparticle-SERS enhancement from silver film over nanosphere (AgFON) substrate. *Plasmonics* **6**(2), 201 (2011).
24. Z. Xu, H-Y. Wu, S.U. Ali, J. Jiang, B.T. Cunningham, and G.L. Liu: Nanoreplicated positive and inverted submicrometer polymer pyramid array for surface-enhanced Raman spectroscopy. *J. Nanophotonics* **5**(1), 053526 (2011).
25. S. Chih-Hung, N.C. Linn, and J. Peng: Templated fabrication of periodic metallic nanopyramid arrays. *Chem. Mater.* **19**(18), 4551 (2007).
26. L. Tzung-Hua, N.C. Linn, L. Tarajano, J. Bin, and J. Peng: Electrochemical SERS at periodic metallic nanopyramid arrays. *J. Phys. Chem. C* **113**(4), 1367 (2009).
27. M. Jin, V. Pully, C. Otto, A. van den Berg, and E.T. Carlen: High-density periodic arrays of self-aligned subwavelength

https://doi.org/10.1557/jmr.2013.352 Published online by Cambridge University Press

nanopyramids for surface-enhanced Raman spectroscopy. *J. Phys. Chem. C* **114**(50), 21953 (2010).
28. Y.J. Liu, H.Y. Chu, and Y.P. Zhao: Silver nanorod array substrates fabricated by oblique angle deposition: Morphological, optical, and SERS characterizations. *J. Phys. Chem. C* **114**(18), 8176 (2010).
29. M. Haiyang, Q. Chuang, L. Pengpeng, and W. Wengang: SERS-active substrates based on metallic nanocracks on PDMS. *Proceedings of the 2011 6th IEEE International Conference on Nano/Micro Engineered and Molecular Systems (NEMS 2011)*, Vol. **321** (2011).
30. A.M. Schwartzberg, C.D. Grant, A. Wolcott, C.E. Talley, T.R. Huser, R. Bogomolni, and J.Z. Zhang: Unique gold nanoparticle aggregates as a highly active surface-enhanced Raman scattering substrate. *J. Phys. Chem. B* **108**(50), 19191 (2004).
31. P.L. Stiles, J.A. Dieringer, N.C. Shah, and R.R. Van Duyne: Surface-enhanced Raman spectroscopy. In *Annual Review of Analytical Chemistry*, 2008; p. 601.
32. Y. Kane: Numerical solution of initial boundary value problems involving Maxwell's equations in isotropic media. *IEEE Antennas Propag.* **14**(3), 302 (1966).
33. E.D. Palik: *Handbook of Optical Constants of Solids: Index* (Elsevier, Philadelphia, PA, 1998).
34. K.C. Vernon, T.J. Davis, F.H. Scholes, D.E. Gomez, and D. Lau: Physical mechanisms behind the SERS enhancement of pyramidal pit substrates. *J. Raman Spectrosc.* **41**(10), 1106 (2010).
35. D. Li, L. Pan, S. Li, K. Liu, S. Wu, and W. Peng: Controlled preparation of uniform TiO_2-catalyzed silver nanoparticle films for surface-enhanced Raman scattering. *J. Phys. Chem. C* **117**(13), 6861 (2013).

Supplementary Material

To view supplementary material for this article, please visit http://dx.doi.org/jmr.2013.352.

https://doi.org/10.1557/jmr.2013.352 Published online by Cambridge University Press